World Journal of Advanced Research and Reviews
eISSN: 2581-9615 CODEN (USA): WJARAI
Cross Ref DOI: 10.30574/wjarr
Journal homepage: https://wjarr.com/

(RESEARCH ARTICLE)

Check for updates

Retention basins for Urban flood mitigation: Insights from Ouagadougou in Burkina Faso

Lawani Adjadi Mounirou [1,*], Roland Yonaba [1], Moussa Diagne Faye [1], Angelbert Chabi Biaou [1], Tazen Fowé [1], Gnenakantanhan Coulibaly [2], Moussa Bruno Kafando [1] and Harouna Karambiri [1]

[1] *Laboratory of Water, Hydro-Systems and Agriculture (LEHSA), International Institute for Water and Environmental Engineering (2iE), PO Box 594, Ouagadougou, Burkina Faso.*
[2] *Joint Engineering Science Research Unit, Geographical Sciences, Civil Engineering and Geosciences Laboratory, Superior School of Public Works (ESTP), Félix Houphouët-Boigny National Polytechnic Institute (INP-HB), PO Box 1093, Yamoussoukro, Côte d'Ivoire.*

World Journal of Advanced Research and Reviews, 2025, 25(01), 1497-1512

Publication history: Received on 06 December 2024; revised on 13 January 2025; accepted on 15 January 2025

Article DOI: https://doi.org/10.30574/wjarr.2025.25.1.0155

Abstract

In this study, we simulated and analyzed the impacts of a retention basin as a hydraulic structure for mitigating flood peaks at the inlet of a stormwater drainage canal using the Storage Indication Curve method for various return periods. The adopted methodology involved modeling the hydraulic behavior of the retention basin and its discharge relationship based on water levels. For initial water levels ranging from 1 to 3 meters in the basin, the effectiveness in reducing peak flows is evaluated by estimating attenuation rates and the temporal delay of flood peaks. The results showed that the performance of the retention basin performance is satisfactory for attenuating a 10-year flood, with attenuation rates ranging from 23% to 54% and a flood peak delay of 20 to 55 minutes. For a 100-year flood, the attenuation rates vary from 18% to 30%, with a peak delay ranging from 17 to 30 minutes, depending on the initial water level. However, for consecutive rainfall events or an initial water level in the basin exceeding 1.5 meters, the hydraulic performance appears limited. Finally, we highlight the limitations of solely relying on retention basins for urban stormwater management and emphasize the need to implement Nature-based Solutions (NbS) at the local level to further mitigate effectively surface runoff in urban settings.

Keywords: Extreme rainfall; Flood hydrograph; Retention basin; Stormwater management; Urban water

1. Introduction

Regional-scale climate changes have been observed in many parts of the world and have already influenced a wide range of physical and biological systems (1). The African continent is particularly vulnerable to the impacts of climate change (2–4). The Sahel region stands out as especially susceptible, both environmentally and socially, and requires special attention as this area has very limited resources to cope with global changes (5–9). Over the past four decades, the West African Sahel has experienced significant climatic fluctuations, notably characterized by an increase in extreme events such as floods (10–13). Many West African cities have faced devastating flood problems with increasing levels of occurrence over the past few decades (14–17). Flooding has submerged entire communities, forcing tens of thousands of families to abandon their homes and belongings for safer locations during the rainy season (18). The Office for the Coordination of Humanitarian Affairs OCHA (19) reported that 2.7 million people have been affected by floods in 2020 in West and Central African countries. Urban centres such as Abidjan (Ivory Coast), Cotonou (Benin), Dakar (Senegal), Lagos (Nigeria), N'Djamena (Chad), Niamey (Niger) and Ouagadougou (Burkina Faso) have suffered considerable damage (2,18,20,21).

* Corresponding author: Lawani Adjadi Mounirou.

The aggravating factors of flood-related damages are associated with intensive and poorly managed urbanization in West African cities (11,18,22), the lack or the aging of sanitation infrastructure (23) and the failures of urban drainage systems (24,25). Poor waste management practices, such as the illegal dumping of solid waste into sewer systems (23), urban agriculture near stormwater drainage channels, dense vegetation in drainage networks, and the increased frequency of extreme rainfall events, further exacerbate these issues (17,26,27). The continuous expansion of traditional drainage systems to mitigate flooding is deemed unsustainable if urbanization and climate change persist (28,29). Therefore, flood risk management is at the intersection of climate dynamics and urbanization processes (30,31).

Ouagadougou, the capital of Burkina Faso, is grappling with an excessive urban expansion due to a high rate of urban growth, driven by population increase, urban migration, and low-density urban development. From an area of 6,860 hectares in 1980, the city now covers 52,000 hectares, representing an eight-fold increase in less than 40 years (32). This expansion has led to the creation of new residential areas, commonly referred to as peripheral neighbourhoods, often located in high-risk zones (e.g., floodplains, marshlands), obstructing natural water flow paths and resulting in a reduction of permeable surfaces. These neighbourhoods house nearly 60% of the urban population, primarily composed of economically and socially vulnerable groups (16,27). Simultaneously, Ouagadougou stormwater drainage networks have not kept pace with urbanization, and existing structures are inadequately maintained (11,27). Moreover, the attitude of some residents, who treat these drainage systems as household waste dumps (23), leads to malfunctioning gutters, hindering water flow during the rainy season. Consequently, the performance of existing structures falls short of expectations due to their inefficiency or incapacity. Added to this are the intense rainfall events, whose frequency and intensity are exacerbated by climate change, amplifying the flood phenomena in major African cities (2,4,33). As a result, flood risks are increasing, and the capacity of drainage networks is becoming inadequate. Floods events are becoming more frequent during the rainy season, causing material damage and sometimes loss of life. Notable examples include the floods in Ouagadougou on September 1, 2009; July 24, 2012; June 24, 2015; September 5, 2020; and August 5, 2022 (11,16,17,27,33,34). These urban floods are a major concern for policymakers, and require a more detailed understanding of these hydrological hazards to effectively manage current and future risks (11,33).

In response to these recurring flood problems, measures for better prevention, management, and risk mitigation are often implemented by municipal authorities, such as the construction of retention basins (35). These hydraulic structures aim to attenuate floods by temporarily storing water volumes to reduce peak flows (36). Several such structures exist in Ouagadougou, including one of the largest, located in the Kouritenga neighbourhood of Sector 29. This retention basin has a storage capacity of 195,000 m^3. However, no prior study assessed the retention basin performance under extreme rainfall events, therefore raising questions about the limitations of existing infrastructure and the need to inform urban planning and current flood risk management practices, especially on practical solutions to enhance resilience in urban settings (16).

This study aims to analyse the effectiveness of these retention basins to mitigate surface runoff and subsequent flooding, as part of urban stormwater management measures. The study uses hydrological and hydraulic modelling to analyse the performance of retention basins in the urban environment of Ouagadougou, considering exceptional rainfall events, of return periods of 10, 50 and 100 years. This study therefore aims to provide critical insights into the effectiveness of retention basins in mitigating urban flood risks, particularly in the context of rapidly urbanizing and climate-vulnerable regions like Ouagadougou, Burkina Faso.

2. Material and methods

2.1. Study area description

This study is conducted in the city of Ouagadougou, focusing on the stormwater retention basin located upstream of the Mogho Naaba canal (12°19'24.02"N, 1°32'21.00"W) (Figure 1). The retention basin drains an upstream area of 354.2 hectares with an average longitudinal slope of 1%. The capital city Ouagadougou, located in central Burkina Faso, is characterized by a Sudano-Sahelian climate and low-permeability ferruginous soils. The climate features a unimodal rainfall pattern with a rainy season from June to October and a dry season from November to May (37,38). The annual precipitation ranges from 588 to 1003 mm, with an interannual average of approximately 783.2 mm over the period 1991–2020 (38). The intensity of some rainfall events, particularly thunderstorms, can reach 110 to 160 mm/h at 5 minutes and 90 mm/h at 30 minutes (39).

Stormwater drainage is managed through primary, secondary, and tertiary pipeline networks. However, this system has demonstrated limitations in both construction and operation. The urban land register of the municipality is divided into two categories: Developed Zones (DZ) and Undeveloped Zones (UZ). DZ are areas that have undergone formal

subdivision and have access to all city services, while UZ are informal settlements. The population of the municipality has significantly increased between 1996 and 2012, doubling from 750,398 inhabitants in 1996 to 1,475,223 in 2006. By 2019, the population was estimated at 2,415,266 inhabitants (32).

Numerous physical and natural factors contribute to the occurrence of floods in Ouagadougou, including soil characteristics, topography, hydrography, and rainfall patterns (11,34,40). The hydrographic network is marked by the presence of three artificial reservoirs (Dams 1, 2, and 3). The terrain is flat, with slopes ranging between 0.5 and 1% (16). As a result, water drainage during the rainy season is challenging due to the low slopes and the encrusted, low-permeability nature of the soils.

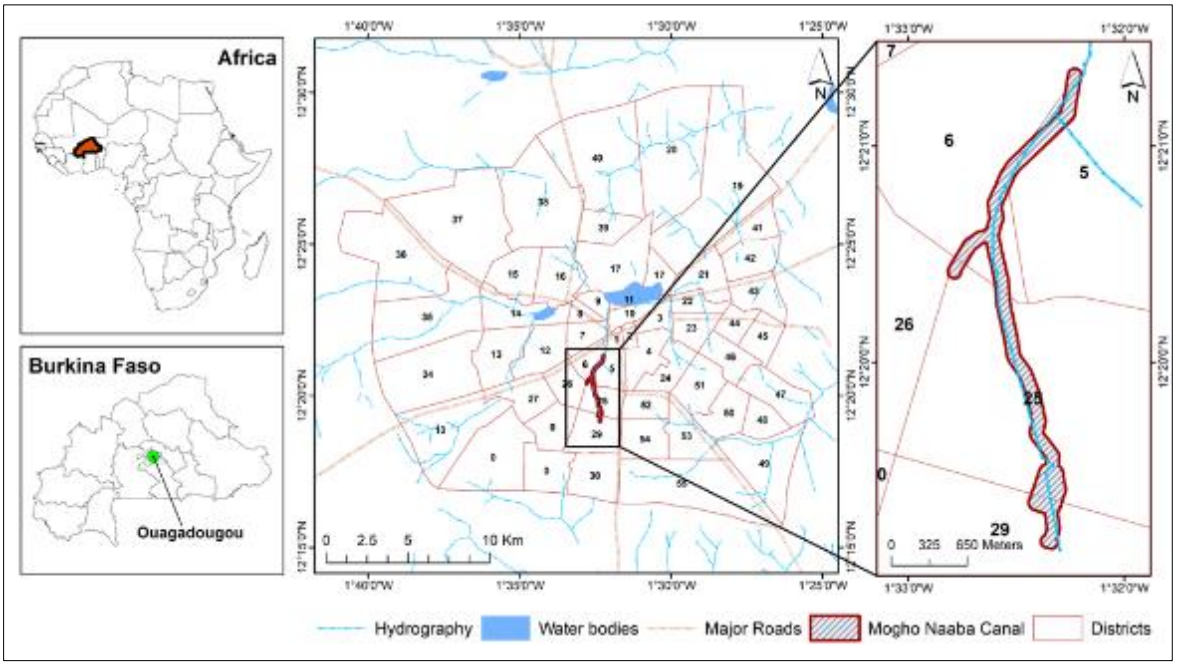

Figure 1 Study area location

2.2. Study area description

This study relies on maximum daily annual rainfall events recorded at the Ouagadougou synoptic station, for the period 1991-2020 (i.e., 30 years). The standard Gumbel distribution (41) is fitted to the dataset to estimate extreme rainfall events of different return periods. The Gumbel distribution is advantageous due to its widespread use in engineering applications in assessing the reliability of hydraulic infrastructure. The return period of an event is defined as the inverse of the annual exceedance probability of that event (42). The cumulative distribution function of the Gumbel distribution is represented by Equation 1

$$F(x; x_0; s) = \exp\left(-\exp\left(\frac{x - x_0}{s}\right)\right) \quad (1)$$

where x_0 is the location parameter and s is the scale factor, both of which are parameters of the distribution. In this study, the Gumbel distribution is applied using the HyfranPlus software (43) while the distribution parameters are estimated using the moments method (44).

2.3. Modelling retention basin

The retention basin cross-section is presented in Figure 2 and has a full capacity of 195,000 m^3. It is 360 meters long and has a trapezoidal shape with an average bottom width of 145 meters and a maximum depth of 3.60 meters. At its downstream end lies a rectangular culvert (4.00 x 4.00 x 2.00 meters) leading into a trapezoidal channel that is 10 meters wide, 1.30 meters high, with side slopes of 1.5. The full-flow discharge capacity of the channel, Q_{2max}, is estimated at 70 m^3 s-1. To enable gravity drainage of the basin, the channel downstream bottom is lowered by 0.20 meters. To optimize basin filling and prevent the premature drainage of initial water inflows, a 2-meter-high and 32-meter-long spillway surrounds the culvert. Three rectangular openings (3.00 x 1.00 x 0.80 meters) act as outlet orifices,

allowing water to drain before it overflows the spillway. The basin's drainage behaviour is governed by the relationships outlined in Equation 2.

$$\begin{cases} If\ h_i \leq h_1 \ \Rightarrow\ Q_i = N \times K_s \times \sqrt{S}\ \dfrac{(b\ \times\ h_i)^{\frac{5}{3}}}{(b + 2\ \times h_i)^{\frac{2}{3}}} \\ If\ 0.8 < h_i \leq h_2 \ \Rightarrow\ Q_i = N\ \times C\ \times (b\ \times\ h_1)\ \times \sqrt{2\,g}\ \times \left(h_i - \dfrac{h_1}{2}\right)^{\frac{1}{2}} \\ If\ h_i \geq 2.0 \ \Rightarrow\ Q_i = Q_{2max} + \mu\ \times\ l_D\ \times \sqrt{2\,g}\ \times (h_i - h_2)^{\frac{3}{2}} \end{cases} \quad (2)$$

where N is the number of rectangular openings, b = 1.0 m is the width of an opening, h_1 = 0.80 m is the height of an opening, K_S = 65 m1/3 s-1 is the Strickler roughness coefficient, $S = 4.4 \times 10^{-3}$ is the basin slope, C = 0.62 is the discharge coefficient of an orifice, h_2 = 2.0 m is the height of the spillway, μ = 0.42 is the discharge coefficient of the spillway, l_D = 32 m is the spillway length and g = 9.81 m s-2 is the gravitational constant due to acceleration.

The water volume in the retention basin is estimated by considering its trapezoidal shape and its geometric dimensions using the relationships described in Equation 3.

$$\begin{cases} If\ h_i \leq H_1 \ \Rightarrow\ S_i = h_i\ \times (b_1 + m_1 \times h_i) \\ If\ h_i > H_1 \ \Rightarrow\ S_i = S_i(H_1) + (h_i - H_1)\big(b_2 + m_2 \times (h_i - H_1)\big) \\ V_i = S_i \times L \end{cases} \quad (3)$$

where b_1 and H_1 are the average width and maximum height of the bottom section of the basin, respectively, b_2 and H_2 are the average width and maximum height of the upper section, respectively, m_1 and m_2 are the side slopes of the two cross-sections, respectively.

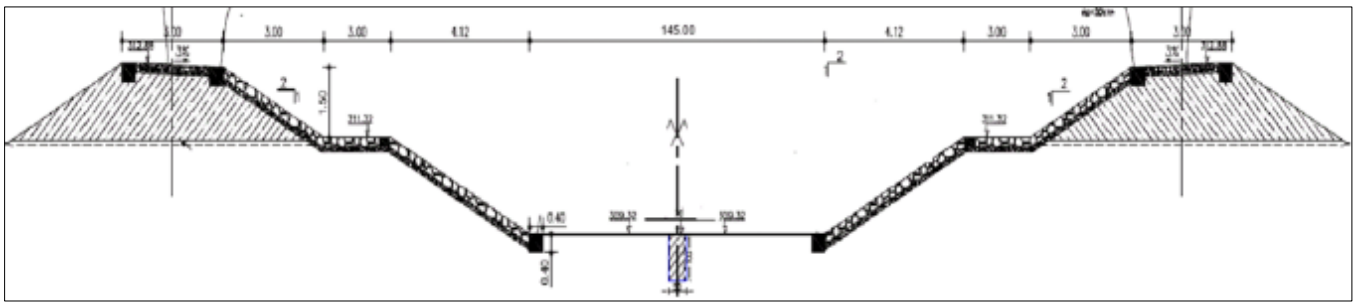

Figure 2 Cross-sectional view of the retention basin in this study

2.4. Coupled hydrological and hydraulic simulation of the retention basin

2.4.1. Definition of a project rainfall shape

The observation data scarcity highly prevalent in Sahel countries, especially Burkina Faso, is challenging of hydrological applications (45,46). In this study, due to the lack of hourly rainfall observations for a typical 10-year rainfall event, we developed a symmetrical double-triangle hyetograph based on Chocat (47). This hyetograph consists of two triangular segments representing an intense rainfall period, respectively preceded and followed by periods of lighter rainfall. This structure is inspired by empirical observations that rain events causing failures in drainage systems typically feature a short duration of intense rainfall, preceded and followed by moderate rainfall (16). This configuration contributes to saturating the storage capacity of the drainage system before the peak rainfall occurs. This typical hyetograph is illustrated in Figure 3.

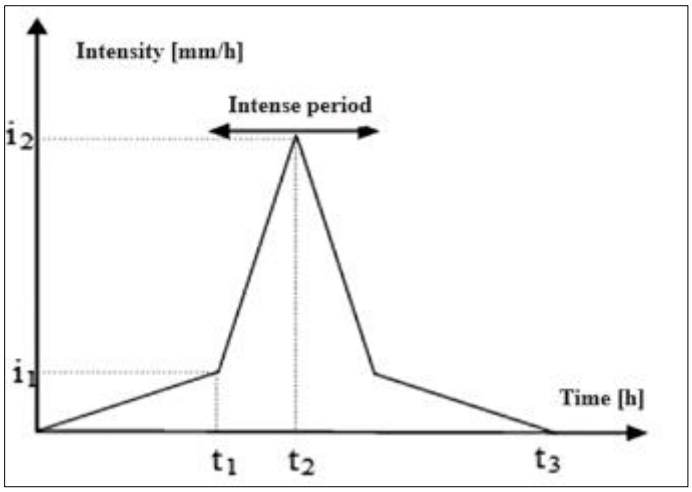

Figure 3 Symmetrical double-triangle hyetograph used in this study. Adapted from Chocat (47)

The double-triangle project rainfall is characterized by the following parameters: t_1 (in minutes, min) is the time at the beginning of the intense period, t_2 (min) is the time at the peak intensity, t_3 (min) is the ending time of the rainfall event, i_1 (mm hr-1) is the rainfall intensity at the beginning of the intense period and i_2 (mm hr-1) is the maximum rainfall intensity.

The rainfall intensities i_1 and i_2 are given by Equation 4.

$$\begin{cases} i_1 = a\ 2^{b+1}\ (0.25\ K)^b\ \dfrac{1 - 0.1^{b+1}}{0.9 \times 0.1^b} \\ i_2 = a\ 2^{b+1}\ (0.25\ K)^b\ \dfrac{0.1^b - 1}{0.9 \times 0.1^b} \end{cases} \quad (4)$$

where a and b are the Montana coefficients for a 10-year return period in the city of Ouagadougou (11,16). The characteristic times of the hyetograph are estimated using Equation 5.

$$t_1 = 2.25K \quad ; \quad t_2 = 2.5K \quad ; \quad t_3 = 5K \quad (5)$$

with K being the response time or lag-time, representing the temporal delay between the centroids of the rainfall and the resulting hydrograph at the watershed outlet. The value of K is estimated using the corrected empirical formula by (48), which is commonly applied in West Africa, as given in Equation 6.

$$K = 3.55 \times A^{0.27} \times (1 + IMP)^{-1.9} \times S^{-0.36} \times T_p^{0.21} \times L^{0.15} \times H_p^{-0.07} \quad (6)$$

where A (ha) is the watershed area, S (%) is the average slope of the watershed, IMP refers to the soil imperviousness coefficient, Tp (min) denotes the duration of the intense rainfall period, L (m) is the length of the main drain channel and Hp (mm) stands for the amount of rainfall fell during Tp.

2.4.2. Inflow hydrograph

Using the previously constructed hyetograph, the Bouvier model (49) is first applied as a production function to derive the net rainfall hyetogram available for runoff. This model includes three parameters: initial losses on permeable surfaces (STO = 8.5 mm), runoff on impermeable surfaces, which is an increasing function of the watershed imperviousness rate (IMP = 55%) and the runoff coefficient for permeable surfaces (C = 40%), which depends on the soil type. After obtaining the net rainfall hyetogram, a linear reservoir model, commonly used in urban hydrology, is employed to generate the hydrograph at the inlet of the retention basin. This model has a single lag-time parameter, K (Equation 6). A time step of 1 minute (Δt = 1 min) is selected, allowing for a reasonably accurate estimation of the instantaneous flow rates. The operating principle is illustrated in Figure 4.

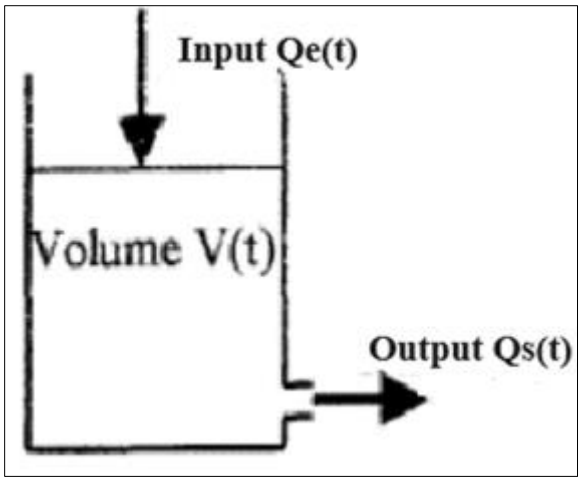

Figure 4 Functioning principle of a linear reservoir model

The variation of the stored volume over time can be expressed as in Equation 7:

$$\frac{dV(t)}{dt} = Q_e(t) - Q_s(t) \tag{7}$$

We introduced Equation 8 for the variation of the stored volume, which depends on the inflow rate $Q_e(t)$ and the outflow rate $Q_s(t)$:

$$V(t) = K[\alpha \times Q_e(t) + (1-\alpha) \times Q_s(t)] \tag{8}$$

where K and α are parameters obtained through calibration. Equation 8 now yields the differential Equation 9:

$$K\alpha \frac{dQ_e(t)}{dt} + K\,(1-\alpha)\frac{dQ_s(t)}{dt} = Q_e(t) - Q_s(t) \tag{9}$$

The resolution of this differential equation through Euler's explicit scheme yield the analytical solution given in Equation 10:

$$Q_s(t+\Delta t) = C_1 \times Q_e(t) + C_2 \times Q_e(t+\Delta t) + C_3 \times Q_s(t) \tag{10}$$

where ⍰t is the integration timestep and C_i coefficients are given by Equation 11:

$$\begin{cases} C_1 = \dfrac{\alpha}{1-\alpha} e^{-\frac{\Delta t}{K(1-\alpha)}} \\ C_2 = 1 - \dfrac{1}{1-\alpha} e^{-\frac{\Delta t}{K(1-\alpha)}} \\ C_3 = e^{-\frac{\Delta t}{K(1-\alpha)}} \end{cases} \tag{11}$$

For a linear reservoir model, the following C_i values given in Equation 12 are obtained:

$$\begin{cases} C_1 = 0 \\ C_2 = 1 - e^{-\frac{\Delta t}{K}} \\ C_3 = e^{-\frac{\Delta t}{K}} \end{cases} \tag{12}$$

2.4.3. Flood Attenuation in the Retention Basin: Storage Indication Curve method

The Storage Indication Curve method (50) is generally recommended for flood attenuation in reservoirs (ref et al.) due to their nonlinear behaviour, as opposed to the Muskingum method (51). This calculation procedure allows for the

determination of the outflow hydrograph of a reservoir given the inflow hydrograph and the reservoir's drainage characteristics. It relies on the discretized form of the continuity equation: the change in storage S between two time points $t = j$ and $t = j + 1$ can be expressed by the relation where O is the outflow rate, I is the inflow rate, and Δt is the time step. The continuity equation is given by Equation 13:

$$\frac{1}{2}\left(I_j + I_{j+1}\right) - \frac{1}{2}\left(O_j + O_{j+1}\right) = \frac{S_{j+1} - S_j}{\Delta t} \tag{13}$$

Re-arranging Equation (13) on both sides yields Equation 14:

$$\left(I_j + I_{j+1}\right) + \left(\frac{2\,S_j}{\Delta t} - O_j\right) = \left(\frac{2\,S_{j+1}}{\Delta t} + O_{j+1}\right) \tag{14}$$

From a curve $\left(\frac{2\,S}{\Delta t} + O\right)$ defined as a function of O, obtained from the height-volume relationship of the retention basin, we calculate O_{j+1}. Then we further evaluate $\left(\frac{2\,S_{j+1}}{\Delta t} - O_{j+1}\right)$ by computing $\left(\frac{2\,S_{j+1}}{\Delta t} + O_{j+1}\right) - 2\,O_{j+1}$. Finally, the computed value of $\left(\frac{2\,S_{j+1}}{\Delta t} - O_{j+1}\right)$ becomes equal to $\left(\frac{2\,S_j}{\Delta t} - O_j\right)$ for the next step.

3. Results

3.1. Rainfall events description

Figure 5 illustrates the key characteristics of annual and daily maximum rainfall over the period 1991-2020. During this observation period, the averages for annual and daily maximum precipitation are 783.2 ± 118.1 mm and 70.9 ± 21.3 mm, respectively. For annual precipitation, the distribution appears to be left-skewed, with a median not centered within the box and higher than the mean. Conversely, for daily maximum precipitation, the median is lower than the mean, and the distribution is skewed towards higher daily maximum precipitation values. While annual precipitation totals seem to be decreasing, the trend for daily maximum precipitation reveals an opposite increasing trend pattern.

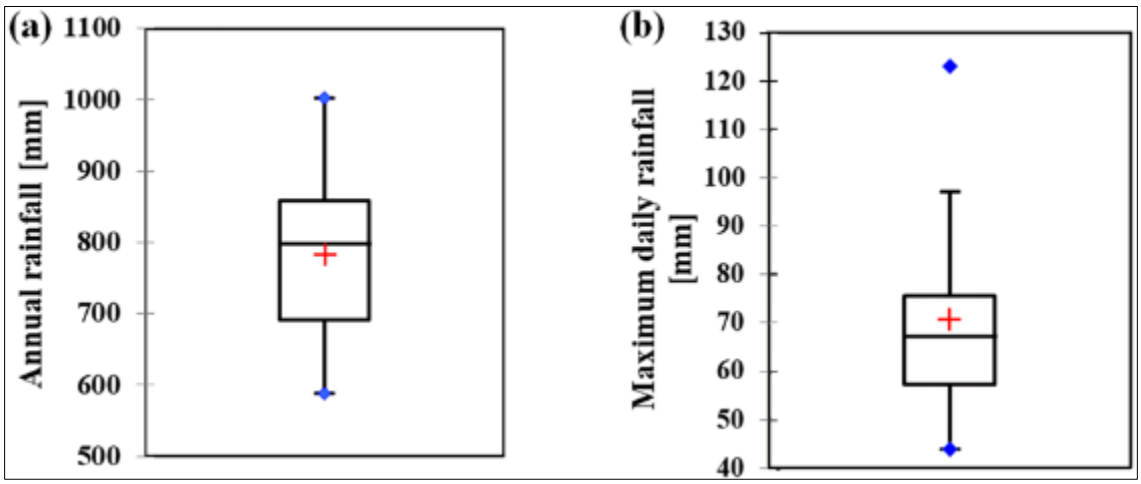

Figure 5 Box plot distributions of annual rainfall (a) and annual daily maximum rainfall (b) in Ouagadougou over the period of 1991-2020

3.2. Extreme value analysis

Several hypothesis tests of independence, homogeneity and stationarity are applied to the annual daily maximum precipitation data from the Ouagadougou synoptic station over the period 1991-2020. Table 1 shows the results of these hypothesis tests, all applied at α = 5% significance level. These results indicate that the timeseries of daily annual maximum rainfall values can be considered independent, homogeneous and stationary values, which makes it eligible to assumptions required for frequency analysis to derive extreme values for further analyses.

Table 1 Statistical tests applied to the daily annual maximum rainfall over the period 1991-2020 at Ouagadougou station.

Hypothesis test	Test statistic	p-value
Wald-Wolfowitz (independence test)	0.328	0.743
Wilcoxon (homogeneity test)	1.590	0.111
Von Neumann (homogeneity test)	1.848	0.336
Mann-Kendall (stationarity test)	1.670	0.096

The significance level applied to all the test is α = 5%.

The fitting of the standard Gumbel distribution to the annual daily maximum precipitation is shown in **Figure 6**. The visual inspection indicates a successful fit, as all observations fall within the 95% confidence band. **Table 2** shows the extreme daily rainfall values derived from the fitting of the Gumbel distribution for various return periods.

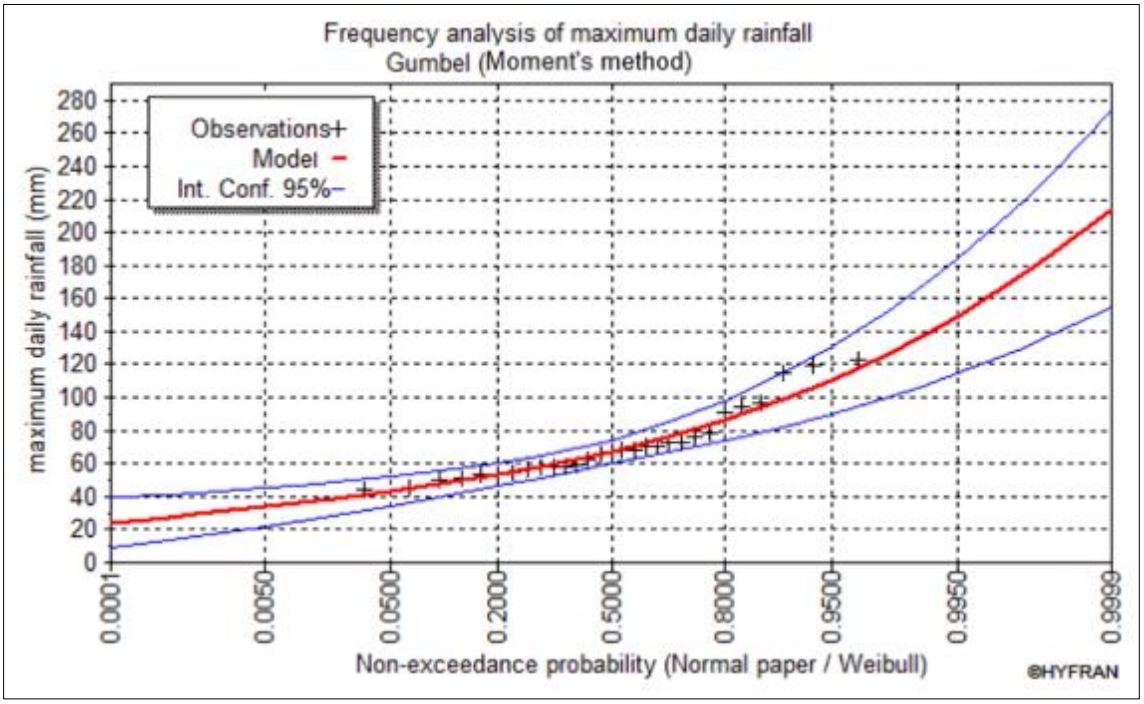

Figure 6 Visual assessment of the fitting of the standard Gumbel distribution to the daily annual maximum rainfall data over the period 1991-2020 at Ouagadougou station

Table 2 Extreme rainfall values derived from Gumbel standard distribution

Return period T [years]	Non-Exceedance probability	Extreme value [mm]	Standard deviation [mm]	Confidence interval [mm]
10	0.90	98.6	8.3	82.4 – 115.0
20	0.95	111.0	10.4	90.1 – 131.0
50	0.98	126.0	13.3	99.9 – 152.0
100	0.99	138.0	15.5	107.0 – 168.0

3.3. Inflow hydrograph

Figure 7 shows the double triangle hyetograph developed for a 10-year design rainfall event superimposed with the hydrograph at the inlet of the retention basin. The characteristics of the upstream watershed (area, average slope, hydraulic length, and imperviousness rate) combined with those of the design rainfall event allowed the estimation of

a lag-time K = 36 min. The hyetograph consists of an intense rainfall period lasting 18 min with a maximum intensity of 248.7 mm hr-1, flanked by two periods of light rainfall lasting around 81 min with a maximum intensity of 39.1 mm hr-1. The rainfall depth during the intense phase is 44 mm, and the total depth of the 10-year rainfall is 96.0 mm. This 10-year rainfall value, calculated using Montana coefficients, appears close to that obtained from the fitting of the standard Gumbel distribution, which is 98.6 mm.

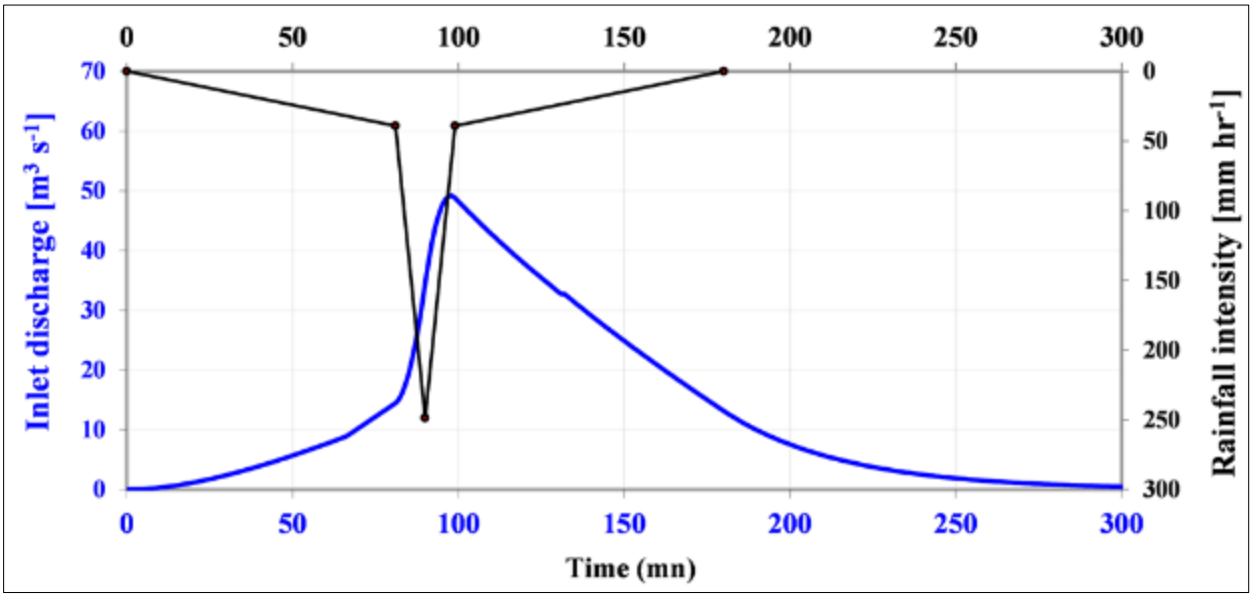

Figure 7 Design inlet hyetograph and hydrograph for a 10-year rainfall event

It is observed that the peak of the rainfall hyetograph occurs approximately 90 min after the onset of rainfall, while the peak of the hydrograph appears at 99 min, i.e. a delay of 9 min. Similarly, the centroids of the hyetograph and hydrograph are approximately at 90 min and 122 min, respectively, indicating that the response time is roughly 32 min. This value closely aligns with that obtained from the empirical estimation (48).

3.4. Flood routing in the retention basin

The hydraulic behaviour of the retention basin is simulated using three types of hydrographs corresponding to rainfall events with return periods of 10, 50 and 100 years, to account for various and increasing associated risks and provide considerations for adapted safety margins. Also, to account for conditions where successive rainfall events occur, the retention basin operation was simulated under various initial water levels, including 0 m, 1 m, 2 m and 3 m (Figure 8).

The simulations show that the retention basin effectively mitigates peak flows, thereby protecting downstream conditions. The different panels in Figure 8 show the effectiveness of flood mitigation by the retention basin. The peak inflow rates of the hydrograph are 49.2 m^3 s-1, 78.7 m^3 s-1, and 98.3 m^3 s-1 for the 10-, 50- and 100-year return periods, respectively.

It is noteworthy that only the peak inflow rate of the 10-year hydrograph is below the full-bank capacity of the downstream channel. Additionally, for an initially empty retention basin, the attenuated hydrograph peaks are 22.6 m^3 s-1, 50.3 m^3 s-1 and 68.8 m^3 s-1 for the 10-, 50- and 100-year return periods, respectively. Moreover, the peak outflow rate of the 100-year flood is lower than the peak inflow rate of the 50-year flood at the entrance of the basin.

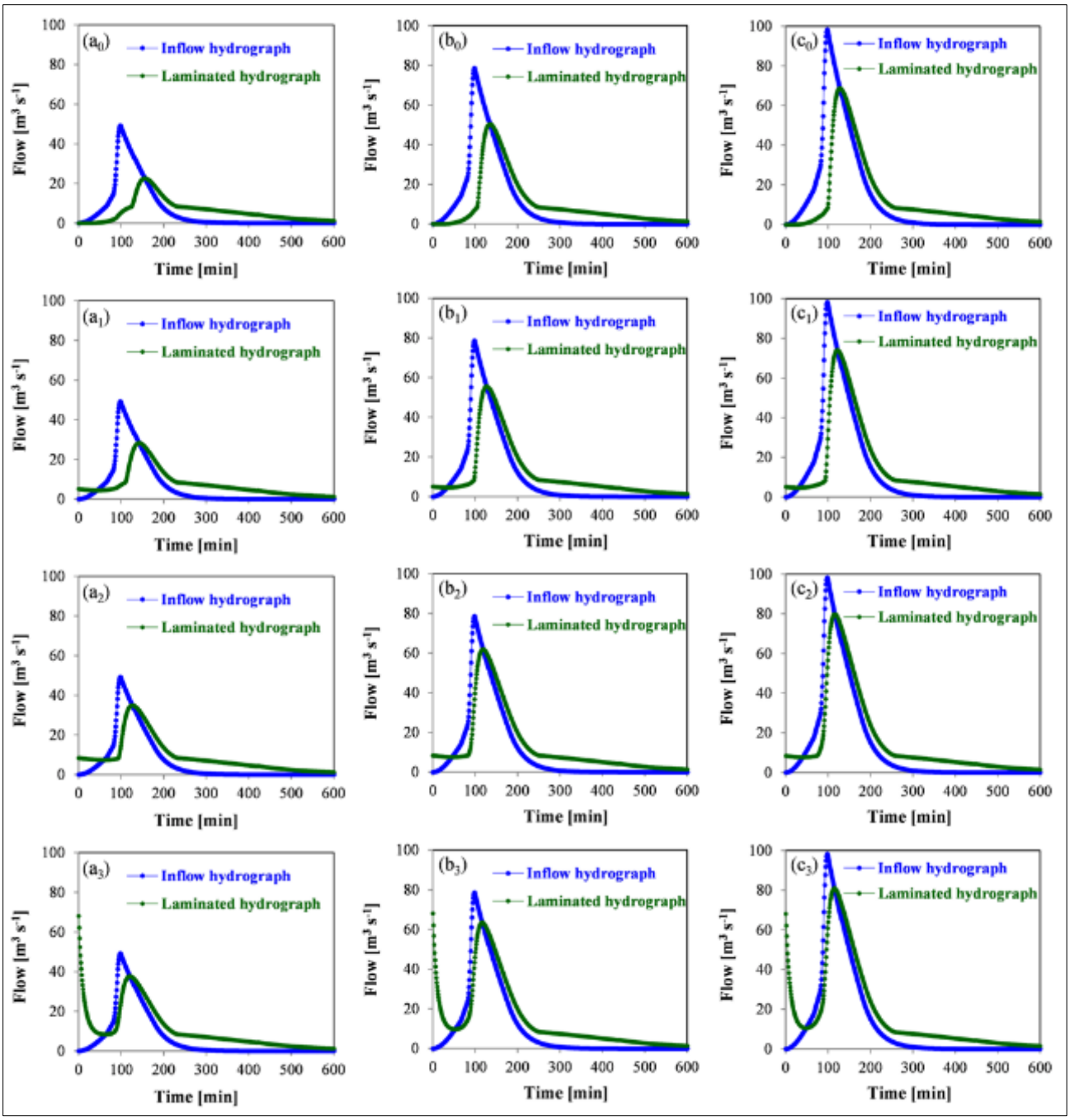

Figure 8 Inflow and laminated hydrograph for various return periods (10-year design rainfall in the first column, 50-year rainfall in the second/middle column and 100-year rainfall in the third/right column). The first row (a0, b0 and c0 panels) shows the hydrographs for an initial water level of 0 m in the retention basin. The second row (a1, b1 and c1 panels) shows the hydrographs for an initial water level of 1 m in the retention basin. The third row (a2, b2 and c2 panels) shows the hydrographs for an initial water level of 2 m in the retention basin. The fourth row (a3, b3 and c3 panels) shows the hydrographs for an initial water level of 3 m in the retention basin

When the retention basin is initially empty, the time lag between the peaks of the hydrographs is 55, 35, and 30 minutes for return periods of 10, 50, and 100 years, respectively. The duration of this lag decreases as the initial water level increases. Additionally, the runoff volume during the 10-year flood is 232,65 m^3, exceeding the maximum capacity of the retention basin. Furthermore, the hydrographs are attenuated to varying degrees depending on the initial water level in the retention basin.

Figure 9 shows the evolution of the attenuation rate of the inflow hydrograph as a function of the initial water level in the retention basin for different return periods. The attenuation rate of a hydrograph varies from 18% to 54%. For a

10-year hydrograph, the attenuation rate ranges from 23% to 54% for an initial water level from 0 to three meters. This rate varies from 18% to 30% for a 100-year hydrograph. When the initial water level in the retention basin is 1.5 m, the attenuation rate for a 10-year flood is the same as that for a 50-year flood with an initially empty basin. Additionally, for initial water levels ≥ 2 m, the attenuation rate seems to stabilize at 18% for both the 50-year and 100-year hydrographs. It can therefore be partially concluded that the performance of the retention basin appears to be satisfactory for attenuating a 10-year flood, even with initial water levels of 1.5 m or less. However, when successive rainfall events occur, the hydraulic performance of the retention basin appears to be limited.

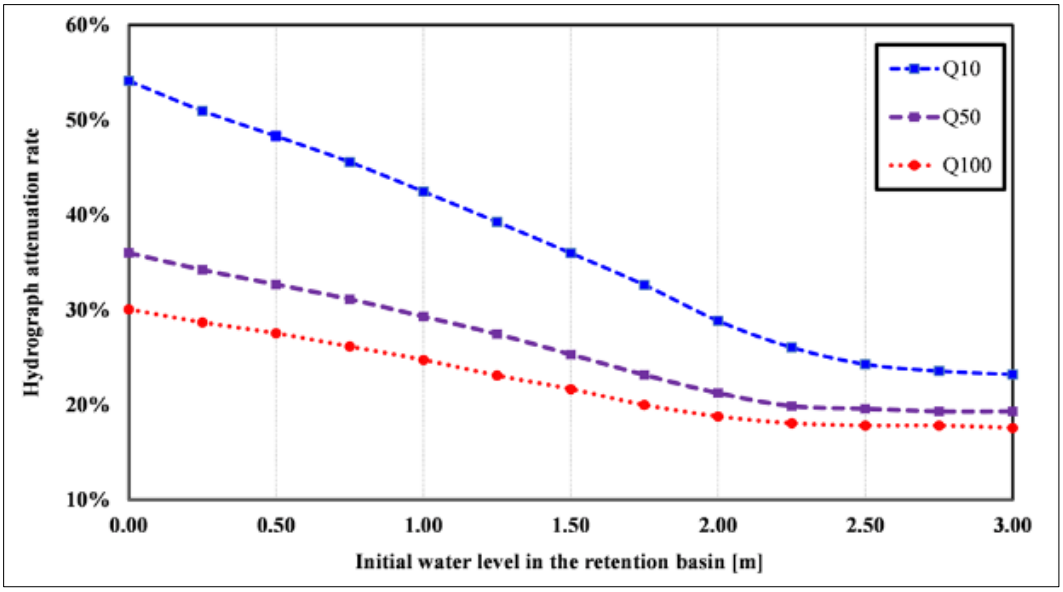

Figure 9 Evolution of the flood hydrograph attenuation rate as a function of the initial water level in the retention basin and the return period

4. Discussion

This study analyzed the effectiveness of a water retention basins to mitigate surface runoff and subsequent flooding in the urban environment of Ouagadougou (capital city of Burkina Faso). The study uses hydrological and hydraulic modelling to analyse the performance and the flood hydrograph attenuation performance for various conditions and increasing return periods of design rainfall events. The findings show that the studied retention basin is effective in managing stormwater generated by rainfall events with a return period below or equal to 10 years. Beyond this threshold, or when successive storms occur, the effectiveness of the retention basin remains marginal. The peak attenuation rates of the hydrographs vary from 18% to 54% for different return periods depending on the initial level. These values are higher than those obtained by Acheampong et al. (52) in the Odaw River basin in Ghana. Also, Emerson et al. (53), in evaluating the effectiveness of an existing stormwater retention basin system operating at the watershed scale, showed that retention basins reduce peak flows at the watershed scale by only 3 to 5%.

Although the usefulness of retention basins is no longer to be demonstrated, their disadvantages are that they constitute solutions to a single problem rather than multiple or cascading problems. For example, retention basins address flooding issues but ignore water quality, wildlife, recreation or aesthetics issues. Moreover, their significant land footprint, associated health risks and drowning risks further limit their development. It has been largely observed that such retention basins are generally used as open air dumpings by local populations during the dry season, which further severely limits their flood attenuation capacity and their functioning for the next wet season (23,54). With the lack of or irregular maintenance, these structures are often silted up by settling sludge, further promoting the development of invasive plant species with the corollary of disrupting proper functioning and reduction of their hydraulic performance.

In the recent years, urban water management have been promoting green stormwater infrastructure and other Nature-based Solutions (NbS) such as wetlands, green roofs, permeable pavements, gardens, and urban green spaces (55,56) to reduce flooding, increase shallow surface water reserves, promote groundwater recharge and improve overall water quality (31). Also, the local-scale development of low-infrastructure development facilities such as trenches, gardens or permeable pavements has been used worldwide as a complement to relieve pressure on urban drainage systems by regulating surface runoff at the source (57).

To enhance the performance of retention basins for higher return periods to allow for containment of future risks, several strategies can be implemented. Increasing the basin size is crucial, as larger dimensions can accommodate larger storm events. Multi-cell designs can improve sedimentation and pollutant removal, with each cell serving a specific function. Extended detention features allow for prolonged water retention, enhancing sedimentation and pollutant removal efficiency, while also improving control of peak flows during significant storm events. Also, designing a meandering flow path can increase the residence time of water within the basin, promoting sedimentation and reducing peak flow rates. Adding features such as aquatic benches can further enhance pollutant removal efficiency by providing additional surface area for sedimentation and biological treatment processes (55).

The study also outlines that operational improvements are also essential. Real-time control systems that respond to current rainfall data can optimize the operation of retention basins, adjusting outlet flows based on conditions to improve flood management and pollutant removal efficiency. Regular maintenance, including sediment removal, vegetation management, and inspection of structural components, is crucial for maintaining optimal performance. Community engagement and education can lead to better stewardship and awareness of the importance of retention basins in urban stormwater management, addressing issues related to solid waste and pollution entering the basins (52,58).

The implementation of these structural enhancements and operational improvements will be key to increase the performance of retention basins, enabling them to better handle higher return periods and contribute effectively to urban stormwater management. These strategies not only enhance hydraulic performance but also improve water quality and ecological benefits, making retention basins a more effective solution for urban environments.

5. Conclusion

This study uses a coupled hydrological and hydraulic modeling chain to evaluate the effectiveness of retention basin for urban flood prevention and management in the urban city of Ouagadougou (Burkina Faso). The covers the definition of a design rainfall event, the transformation of a rainfall hyetograph into a flood hydrograph through empirical production and transfer functions. Three return periods (10-, 50- and 100-year) for design rainfall events and various initial water level conditions (0 m, 1 m, 2 m and 3 m) in the retention basin were considered to assess the hydraulic performance and flood attenuation rate capabilities of the retention basin. The study showed that the retention basin significantly mitigates flood inlet hydrographs by reducing the flood peak, with a time lag of 30 to 55 minutes in peak discharge depending on the return period of the rainfall event. For a 10-year design rainfall, the peak attenuation rate of the hydrographs varies from 23% to 54% for initial water level between 0-3 m. This rate varies from 18% to 30% for a 100-year hydrograph under the same initial water level conditions. The study concludes that although retention basins are widely used worldwide for urban flood prevention and management, they appear limited in terms of ability to handle increasing incoming runoff in the case of higher rainfall events, which are becoming more common due to climate change effects. Moreover, their large footprint, and associated risks limit their development, raising the need to combine retention basins with green infrastructure and adapt their sizing approaches.

Compliance with ethical standards

Disclosure of conflict of interest

The authors have no relevant financial or non-financial interests to disclose.

Data Availability

All the data (raw or generated) used during the study are available upon reasonable request from the corresponding author.

Funding

This research did not receive any specific grant from funding agencies in the public, commercial, or not-for-profit sectors.

Author contributions

All authors contributed to the study conception and design. Material preparation, data collection and analysis were performed by Lawani Adjadi Mounirou, Roland Yonaba and Moussa Diagne Faye. The first draft of the manuscript was

written by Lawani Adjadi Mounirou and Roland Yonaba. All authors commented on previous versions of the manuscript. All authors read and approved the final manuscript.

References

[1] Calvin K, Dasgupta D, Krinner G, Mukherji A, Thorne PW, Trisos C, et al. IPCC, 2023: Climate Change 2023: Synthesis Report. Contribution of Working Groups I, II and III to the Sixth Assessment Report of the Intergovernmental Panel on Climate Change [Core Writing Team, H. Lee and J. Romero (eds.)]. IPCC, Geneva, Switzerland. [Internet]. First. Intergovernmental Panel on Climate Change (IPCC); 2023 juill [cité 24 août 2024]. Disponible sur: https://www.ipcc.ch/report/ar6/syr/

[2] Taylor CM, Belušić D, Guichard F, Parker DJ, Vischel T, Bock O, et al. Frequency of extreme Sahelian storms tripled since 1982 in satellite observations. Nature [Internet]. avr 2017 [cité 4 févr 2020];544(7651):475-8. Disponible sur: http://www.nature.com/articles/nature22069

[3] Panthou G, Lebel T, Vischel T, Quantin G, Sane Y, Ba A, et al. Rainfall intensification in tropical semi-arid regions: the Sahelian case. Environmental Research Letters [Internet]. juin 2018 [cité 4 févr 2020];13(6):064013. Disponible sur: http://stacks.iop.org/1748-9326/13/i=6/a=064013?key=crossref.97be9943c78ecacff82b3dcfa3e9c171

[4] Yonaba R, Mounirou LA, Tazen F, Koïta M, Biaou AC, Zouré CO, et al. Future climate or land use? Attribution of changes in surface runoff in a typical Sahelian landscape. Comptes Rendus Géoscience [Internet]. 12 janv 2023 [cité 13 janv 2023];355(S1):1-28. Disponible sur: https://comptes-rendus.academie-sciences.fr/geoscience/articles/10.5802/crgeos.179/

[5] Gbohoui YP, Paturel JE, Fowe Tazen, Mounirou LA, Yonaba R, Karambiri H, et al. Impacts of climate and environmental changes on water resources: A multi-scale study based on Nakanbé nested watersheds in West African Sahel. Journal of Hydrology: Regional Studies [Internet]. juin 2021 [cité 22 juin 2022];35:100828. Disponible sur: https://linkinghub.elsevier.com/retrieve/pii/S2214581821000574

[6] Lèye B, Zouré CO, Yonaba R, Karambiri H. Water Resources in the Sahel and Adaptation of Agriculture to Climate Change: Burkina Faso. In: Diop S, Scheren P, Niang A, éditeurs. Climate Change and Water Resources in Africa [Internet]. Cham: Springer International Publishing; 2021 [cité 29 juill 2024]. p. 309-31. Disponible sur: http://link.springer.com/10.1007/978-3-030-61225-2_14

[7] Yonaba R, Koïta M, Mounirou LA, Tazen F, Queloz P, Biaou AC, et al. Spatial and transient modelling of land use/land cover (LULC) dynamics in a Sahelian landscape under semi-arid climate in northern Burkina Faso. Land Use Policy [Internet]. avr 2021 [cité 29 juill 2024];103:105305. Disponible sur: https://linkinghub.elsevier.com/retrieve/pii/S0264837721000284

[8] Mounirou LA, Yonaba R, Tazen F, Ayele GT, Yaseen ZM, Karambiri H, et al. Soil Erosion across Scales: Assessing Its Sources of Variation in Sahelian Landscapes under Semi-Arid Climate. Land [Internet]. 15 déc 2022 [cité 29 juill 2024];11(12):2302. Disponible sur: https://www.mdpi.com/2073-445X/11/12/2302

[9] Nkiaka E, Bryant RG, Dembélé M, Yonaba R, Priscilla AI, Karambiri H. Quantifying the effects of climate and environmental changes on evapotranspiration variability in the Sahel. Journal of Hydrology [Internet]. 2024;131874. Disponible sur: https://www.sciencedirect.com/science/article/pii/S0022169424012708

[10] Wilcox C, Vischel T, Panthou G, Bodian A, Blanchet J, Descroix L, et al. Trends in hydrological extremes in the Senegal and Niger Rivers. Journal of Hydrology [Internet]. nov 2018 [cité 11 janv 2024];566:531-45. Disponible sur: https://linkinghub.elsevier.com/retrieve/pii/S0022169418305766

[11] Fowé T, Diarra A, Kabore RFW, Ibrahim B, Bologo/Traoré M, Traoré K, et al. Trends in flood events and their relationship to extreme rainfall in an urban area of Sahelian West Africa: The case study of Ouagadougou, Burkina Faso. Journal of Flood Risk Management [Internet]. oct 2019 [cité 4 févr 2020];12(S1). Disponible sur: https://onlinelibrary.wiley.com/doi/abs/10.1111/jfr3.12507

[12] Sagna P, Dipama JM, Vissin EW, Diomandé BI, Diop C, Chabi PAB, et al. Climate Change and Water Resources in West Africa: A Case Study of Ivory Coast, Benin, Burkina Faso, and Senegal. In: Diop S, Scheren P, Niang A, éditeurs. Climate Change and Water Resources in Africa [Internet]. Cham: Springer International Publishing; 2021 [cité 1 juin 2023]. p. 55-86. Disponible sur: http://link.springer.com/10.1007/978-3-030-61225-2_4

[13] Yonaba R, Biaou AC, Koïta M, Tazen F, Mounirou LA, Zouré CO, et al. A dynamic land use/land cover input helps in picturing the Sahelian paradox: Assessing variability and attribution of changes in surface runoff in a Sahelian

watershed. Science of The Total Environment [Internet]. févr 2021 [cité 28 juill 2024];757:143792. Disponible sur: https://linkinghub.elsevier.com/retrieve/pii/S004896972037323X

[14] Hangnon H, De Longueville F, Ozer P. Précipitations 'extrêmes' et inondations à Ouagadougou ; quand le développement urbain est mal maîtrisé... In ULg - Université de Liège; 2015 [cité 1 janv 2015]. p. 497. Disponible sur: http://www.climato.be/aic/colloques/actes/ACTES_AIC2015/5%20Variabilites%20et%20aleas%20climatiques/080-HANGNON-497-502.pdf

[15] Singh P, Sinha VSP, Vijhani A, Pahuja N. Vulnerability assessment of urban road network from urban flood. International Journal of Disaster Risk Reduction [Internet]. juin 2018 [cité 24 août 2024];28:237-50. Disponible sur: https://linkinghub.elsevier.com/retrieve/pii/S2212420918303261

[16] Coulibaly G, Leye B, Tazen F, Mounirou LA, Karambiri H. Urban Flood Modeling Using 2D Shallow-Water Equations in Ouagadougou, Burkina Faso. Water [Internet]. 26 juill 2020 [cité 16 nov 2023];12(8):2120. Disponible sur: https://www.mdpi.com/2073-4441/12/8/2120

[17] Da MLC, Hangnon H, Amalric M, Nikiema A, Robert E, Bonnet E. Revealing social vulnerability profiles for urban flood management: the case of Ouagadougou (Burkina Faso). cybergeo [Internet]. 12 févr 2022 [cité 24 août 2024]; Disponible sur: http://journals.openedition.org/cybergeo/38243

[18] Souley Tangam I, Yonaba R, Niang D, Adamou MM, Keïta A, Karambiri H. Daily Simulation of the Rainfall–Runoff Relationship in the Sirba River Basin in West Africa: Insights from the HEC-HMS Model. Hydrology [Internet]. 28 févr 2024 [cité 29 juill 2024];11(3):34. Disponible sur: https://www.mdpi.com/2306-5338/11/3/34

[19] OCHA. West and Central Africa: Flooding Situation As of 10 October 2020 - Niger | ReliefWeb [Internet]. UN Office for the Coordination of Humanitarian Affairs (OCHA); 2020 [cité 24 août 2024]. Disponible sur: https://reliefweb.int/report/niger/west-and-central-africa-flooding-situation-10-october-2020

[20] Bouly S, Cisse A, Faye C. Problematic of storm water management in cities in developing countries: case of Santhiaba and Belfort district (commune of Ziguinchor, Senegal). LARHYSS Journal [Internet]. 2019;(39):313-31. Disponible sur: http://www.larhyss.net/ojs/index.php/larhyss/article/view/683/0

[21] Hountondji B, CODO F, DAHOUNTO S, GBAGUIDI T. Flood management in urban environment: case of the Cotonou city in Benin. LARHYSS Journal [Internet]. 2019;(39):333-47. Disponible sur: http://larhyss.net/ojs/index.php/larhyss/article/view/693

[22] Hassan BT, Yassine M, Amin D. Comparison of Urbanization, Climate Change, and Drainage Design Impacts on Urban Flashfloods in an Arid Region: Case Study, New Cairo, Egypt. Water [Internet]. 5 août 2022 [cité 24 août 2024];14(15):2430. Disponible sur: https://www.mdpi.com/2073-4441/14/15/2430

[23] Zoungrana M, Andrianisa HA, Yonaba R, Mabia AG, Thiam S, Bonkian B. A GIS-based approach for improving urban sanitation planning and services delivery: A case study from Ouagadougou, Burkina Faso. Habitat International. 2024;143(102993).

[24] Ouattara ZA, Kabo-Bah AT, Dongo K, Akpoti K. A Review of sewerage and drainage systems typologies with case study in Abidjan, Côte d'Ivoire: failures, policy and management techniques perspectives. Cogent Engineering [Internet]. 31 déc 2023 [cité 24 août 2024];10(1):2178125. Disponible sur: https://www.tandfonline.com/doi/full/10.1080/23311916.2023.2178125

[25] Chen T, Chen L, Shao Z, Chai H. Enhanced resilience in urban stormwater management through model predictive control and optimal layout schemes under extreme rainfall events. Journal of Environmental Management [Internet]. août 2024 [cité 24 août 2024];366:121767. Disponible sur: https://linkinghub.elsevier.com/retrieve/pii/S0301479724017535

[26] Descroix L, Guichard F, Grippa M, Lambert L, Panthou G, Mahé G, et al. Evolution of Surface Hydrology in the Sahelo-Sudanian Strip: An Updated Review. Water [Internet]. juin 2018 [cité 20 juin 2019];10(6):748. Disponible sur: http://www.mdpi.com/2073-4441/10/6/748

[27] Schlef KE, Kaboré L, Karambiri H, Yang YCE, Brown CM. Relating perceptions of flood risk and coping ability to mitigation behavior in West Africa: Case study of Burkina Faso. Environmental Science & Policy [Internet]. nov 2018 [cité 24 août 2024];89:254-65. Disponible sur: https://linkinghub.elsevier.com/retrieve/pii/S1462901118300327

[28] Dong X, Guo H, Zeng S. Enhancing future resilience in urban drainage system: Green versus grey infrastructure. Water Research [Internet]. nov 2017 [cité 24 août 2024];124:280-9. Disponible sur: https://linkinghub.elsevier.com/retrieve/pii/S0043135417306115

[29] Liang R, Di Matteo M, Maier H, Thyer M. Real-Time, Smart Rainwater Storage Systems: Potential Solution to Mitigate Urban Flooding. Water [Internet]. 20 nov 2019 [cité 24 août 2024];11(12):2428. Disponible sur: https://www.mdpi.com/2073-4441/11/12/2428

[30] Sadeghi KM, Loáiciga HA, Kharaghani S. Stormwater Control Measures for Runoff and Water Quality Management in Urban Landscapes. J American Water Resour Assoc [Internet]. févr 2018 [cité 24 août 2024];54(1):124-33. Disponible sur: https://onlinelibrary.wiley.com/doi/10.1111/1752-1688.12547

[31] Shishegar S, Duchesne S, Pelletier G. Optimization methods applied to stormwater management problems: a review. Urban Water Journal [Internet]. 16 mars 2018 [cité 24 août 2024];15(3):276-86. Disponible sur: https://www.tandfonline.com/doi/full/10.1080/1573062X.2018.1439976

[32] INSD. 5th General Census of Population and Housing in Burkina Faso (5ème Recensement Général de la Population et de l'Habitation du Burkina Faso) [Internet]. Ouagadougou, Burkina Faso: Comité National du Recensement Institut National de la Statistique et de la Démographie; 2022 p. 136. Disponible sur: http://cns.bf/IMG/pdf/plaquette_resultats_definitifs_rgph_2019_-_revu_30-12-2022.pdf

[33] Miller JD, Vischel T, Fowe T, Panthou G, Wilcox C, Taylor CM, et al. A modelling-chain linking climate science and decision-makers for future urban flood management in West Africa. Reg Environ Change [Internet]. sept 2022 [cité 24 août 2024];22(3):93. Disponible sur: https://link.springer.com/10.1007/s10113-022-01943-x

[34] Bouvier C, Chahinian N, Adamovic M, Cassé C, Crespy A, Crès A, et al. Large-Scale GIS-Based Urban Flood Modelling: A Case Study on the City of Ouagadougou. In: Gourbesville P, Cunge J, Caignaert G, éditeurs. Advances in Hydroinformatics [Internet]. Singapore: Springer Singapore; 2018 [cité 24 août 2024]. p. 703-17. (Springer Water). Disponible sur: http://link.springer.com/10.1007/978-981-10-7218-5_50

[35] Bustami RA, Bong CHJ, Mah DYS, Hamzah AAA, Patrick M. Modeling of Flood Mitigation Structures for Sarawak River Sub-basin Using Info Works River Simulation (RS). Journal of Civil and Environmental Engineering [Internet]. 2009;3:248-52. Disponible sur: https://api.semanticscholar.org/CorpusID:15054361

[36] Yuan S, Li Z, Li P, Xu G, Gao H, Xiao L, et al. Influence of Check Dams on Flood and Erosion Dynamic Processes of a Small Watershed in the Loss Plateau. Water [Internet]. 19 avr 2019 [cité 24 août 2024];11(4):834. Disponible sur: https://www.mdpi.com/2073-4441/11/4/834

[37] Mounirou LA, Sawadogo B, Yanogo H, Yonaba R, Zorom M, Faye MD, et al. Estimation of the Actual Specific Consumption in Drinking Water Supply Systems in Burkina Faso (West Africa): Potential Implications for Infrastructure Sizing. Water [Internet]. 28 sept 2023 [cité 16 mars 2024];15(19):3423. Disponible sur: https://www.mdpi.com/2073-4441/15/19/3423

[38] Yonaba R, Tazen F, Cissé M, Mounirou LA, Belemtougri A, Ouedraogo VA, et al. Trends, sensitivity and estimation of daily reference evapotranspiration ET0 using limited climate data: regional focus on Burkina Faso in the West African Sahel. Theor Appl Climatol [Internet]. juill 2023 [cité 16 mars 2024];153(1-2):947-74. Disponible sur: https://link.springer.com/10.1007/s00704-023-04507-z

[39] Mounirou LA, Yonaba R, Koïta M, Paturel JE, Mahé G, Yacouba H, et al. Hydrologic similarity: dimensionless runoff indices across scales in a semi-arid catchment. Journal of Arid Environments [Internet]. oct 2021 [cité 22 juin 2022];193:104590. Disponible sur: https://linkinghub.elsevier.com/retrieve/pii/S0140196321001567

[40] Engel T, Fink AH, Knippertz P, Pante G, Bliefernicht J. Extreme Precipitation in the West African Cities of Dakar and Ouagadougou: Atmospheric Dynamics and Implications for Flood Risk Assessments. Journal of Hydrometeorology [Internet]. 1 nov 2017 [cité 24 août 2024];18(11):2937-57. Disponible sur: http://journals.ametsoc.org/doi/10.1175/JHM-D-16-0218.1

[41] Gumbel EJ. Statistics of Extremes [Internet]. Columbia University Press; 1958 [cité 24 août 2024]. Disponible sur: https://www.degruyter.com/document/doi/10.7312/gumb92958/html

[42] Mohymont B, Demarée GR. Courbes intensité—durée—fréquence des précipitations à Yangambi, Congo, au moyen de différents modèles de type Montana. Hydrological Sciences Journal [Internet]. avr 2006 [cité 24 août 2024];51(2):239-53. Disponible sur: https://www.tandfonline.com/doi/full/10.1623/hysj.51.2.239

[43] INRS-ETE. HYFRAN-PLUS [Internet]. France: INRS-ETE; 2021. Disponible sur: https://www.wrpllc.com/books/HyfranPlus/hyfranplusgeneralinfo.html

[44] Hosking JRM. L-Moments: Analysis and Estimation of Distributions Using Linear Combinations of Order Statistics. Journal of the Royal Statistical Society Series B: Statistical Methodology [Internet]. 1 sept 1990 [cité 25 août 2024];52(1):105-24. Disponible sur: https://academic.oup.com/jrsssb/article/52/1/105/7027905

[45] Yonaba R, Belemtougri A, Fowé T, Mounirou LA, Nkiaka E, Dembélé M, et al. Rainfall estimation in the West African Sahel: comparison and cross-validation of top-down vs. bottom-up precipitation products in Burkina Faso. Geocarto International [Internet]. janv 2024 [cité 19 août 2024];39(1):2391956. Disponible sur: https://www.tandfonline.com/doi/full/10.1080/10106049.2024.2391956

[46] Yonaba R, Mounirou LA, Keïta A, Fowé T, Zouré CO, Belemtougri A, et al. Exploring the Added Value of Sub-Daily Bias Correction of High-Resolution Gridded Rainfall Datasets for Rainfall Erosivity Estimation. Hydrology [Internet]. 23 août 2024 [cité 24 août 2024];11(9):132. Disponible sur: https://www.mdpi.com/2306-5338/11/9/132

[47] Chocat B. Encyclopédie de l'hydrologie urbaine et de l'assainissement. Londres Paris New York: Tec & doc-Lavoisier; 1997.

[48] Desbordes M. Réflexions sur les méthodes de calcul des réseaux urbains d'assainissement pluvial [Internet]. Université des Sciences et Techniques du Languedoc; 1974. Disponible sur: https://books.google.bf/books?id=6EsAnwEACAAJ

[49] Bouvier C, Desbordes M. Un modèle de ruissellement urbain pour les villes d'Afrique de l'Ouest. Hydrologie continentale [Internet]. 1990;5(2):77-86. Disponible sur: https://pascal-francis.inist.fr/vibad/index.php?action=getRecordDetail&idt=19728520

[50] Joseph AP. Storage Indication Method of Flood Routing for Design of Small Detention and Storage Dams. Water and Energy International. 1962;19(12):997-1002.

[51] Song X meng, Kong F zhe, Zhu Z xia. Application of Muskingum routing method with variable parameters in ungauged basin. Water Science and Engineering. 2011;4(1):1-12.

[52] Acheampong JN, Gyamfi C, Arthur E. Impacts of retention basins on downstream flood peak attenuation in the Odaw river basin, Ghana. Journal of Hydrology: Regional Studies [Internet]. juin 2023 [cité 24 août 2024];47:101364. Disponible sur: https://linkinghub.elsevier.com/retrieve/pii/S2214581823000514

[53] Emerson CH, Welty C, Traver RG. Watershed-Scale Evaluation of a System of Storm Water Detention Basins. J Hydrol Eng [Internet]. mai 2005 [cité 24 août 2024];10(3):237-42. Disponible sur: https://ascelibrary.org/doi/10.1061/%28ASCE%291084-0699%282005%2910%3A3%28237%29

[54] Loukil F, Rouached L. Waste collection criticality index in African cities. Waste Management [Internet]. févr 2020 [cité 24 août 2024];103:187-97. Disponible sur: https://linkinghub.elsevier.com/retrieve/pii/S0956053X19307810

[55] Dhakal KP, Chevalier LR. Urban Stormwater Governance: The Need for a Paradigm Shift. Environmental Management [Internet]. mai 2016 [cité 24 août 2024];57(5):1112-24. Disponible sur: http://link.springer.com/10.1007/s00267-016-0667-5

[56] Prudencio L, Null SE. Stormwater management and ecosystem services: a review. Environ Res Lett [Internet]. 1 mars 2018 [cité 24 août 2024];13(3):033002. Disponible sur: https://iopscience.iop.org/article/10.1088/1748-9326/aaa81a

[57] Li C, Peng C, Chiang PC, Cai Y, Wang X, Yang Z. Mechanisms and applications of green infrastructure practices for stormwater control: A review. Journal of Hydrology [Internet]. janv 2019 [cité 24 août 2024];568:626-37. Disponible sur: https://linkinghub.elsevier.com/retrieve/pii/S0022169418308539

[58] Abduljaleel Y, Salem A, Ul Haq F, Awad A, Amiri M. Improving detention ponds for effective stormwater management and water quality enhancement under future climate change: a simulation study using the PCSWMM model. Sci Rep [Internet]. 5 avr 2023 [cité 24 août 2024];13(1):5555. Disponible sur: https://www.nature.com/articles/s41598-023-32556-x